IEEE Access
Multidisciplinary | Rapid Review | Open Access Journal

Received June 14, 2019, accepted June 23, 2019, date of publication July 10, 2019, date of current version July 29, 2019.

Digital Object Identifier 10.1109/ACCESS.2019.2927817

Trajectory Optimization and Finite-Time Control for Unmanned Helicopters Formation

BOYUAN ZHANG, QUN ZONG, (Member, IEEE), LIQIAN DOU, BAILING TIAN, (Member, IEEE), DANDAN WANG, AND XINYI ZHAO

School of Electrical Automation and Information Engineering, Tianjin University, Tianjin 300071, China

Corresponding author: Liqian Dou (douliqian@tju.edu.cn)

This work was supported in part by the National Natural Science Foundation of China under Grant 61673294, Grant 61573060, Grant 61503323, Grant 61773278, and Grant 61703134.

ABSTRACT A safe and rapid formation generation is of great importance for the cooperation performance of the multiple unmanned helicopters. The trajectory optimization and control is the key problem in the process of the formation generation. To achieve this goal, a novel safe formation generation strategy is proposed through trajectory optimization and tracking control. First, the rapidly-exploring random tree (RRT) algorithm is applied to obtain the initial guess to satisfy the requirement of rapid solution. Then, the Gauss pseudospectral method is used to transform the optimal control problem to the nonlinear programming (NLP) problem and the sequence quadratic programming (SQP) method is utilized to gain the optimal trajectory combined with the initial guess. Second, a finite-time sliding mode controller is proposed to ensure the finite time trajectory tracking in the presence of model parameter uncertainties and unknown external disturbances. Finally, the numerical simulation is provided to show the effectiveness of the proposed formation generation strategy for unmanned helicopters formation.

INDEX TERMS Trajectory optimization, finite-time sliding mode controller, unmanned helicopters formation.

I. INTRODUCTION

With the vertical takeoff, landing, air hovering and flexible flight characteristics, unmanned helicopter has been widely used in military and civilian fields, such as target reconnaissance, disaster relief, strike power patrols and agricultural plant protection [1]–[4]. With the increase of task complexity and number, a single unmanned helicopter is hardly to satisfy the requirements. Hence, the interest in multiple unmanned helicopters has been growing strongly. The collaborative unmanned helicopters can improve the mission efficiency, flexibility and fault tolerance [5]. It should be noted that formation generation is an essential part in the process of collaboration and rapid formation generation will improve the mission efficiency and flight safety.

Therefore, it is of great significance to study the formation generation of unmanned helicopters formation. The main challenge is to guarantee the safe and rapid performance in the presence of external disturbance and model uncertainty.

The associate editor coordinating the review of this manuscript and approving it for publication was Bin Xu.

The problem is solved through trajectory optimization and finite-time control in this paper. The trajectory optimization methods are mainly divided into two categories: indirect methods and direct methods [6], [7]. The trajectory optimization problem with boundary value and path constraints was converted into a Hamiltonian two-point boundary value problem by indirect method which satisfied the first-order necessary condition using the minimum principle [8]. The indirect method involving trim-reference functions was used to gain the optimal path for unmanned aerial vehicle (UAV) by Barron and Chick [9]. The direct and indirect methods were employed to compute feedforward control sequences for the flight control of a quadrotor UAV and optimization results were compared with respect to the accuracy and applicability [10]. The trajectory gained by indirect method had a high accuracy with the disadvantage of the initial values sensitivity, low convergence speed and small convergence domain. The optimization research mainly concentrated on the direct method. Direct collocation method was used to solve the trajectory optimization problem for spacecraft proximity rendezvous with path constraints by Liu [11].

Numerical simulation results demonstrated that the proposed method was not sensitive to the initial condition, however the solution speed does not meet the real-time requirements. The trajectory of a tubular launched cruising unmanned aerial vehicle was optimized using the modified direct collocation method for attacking a target at back slope under a wind gradient by Jiang, but the result could be only applied for a single UAV [12]. Taking into account the problems of traditional direct and indirect methods, the pseudospectral technique was proposed to solve the trajectory optimization problems [10].

The pseudospectral method, as an effective direct method, has attracted a lot of attention in recent 20 years. It has larger convergence region and faster convergence speed by combining the advantages of indirect method and direct method [13]. Pseudospectral method has been sussessfully applied in engineering practice due to the effectiveness and rapidity. The team of Ross [14] realized the optimization of large-angle attitude maneuver of the International Space Station under ''zero fuel'' using self-developed DIDO pseudospectral optimization software package, which verified the feasibility of the method. The pseudospectral solver was used to gain the optimal trajectory for an UAV in the presence of a wind field. The simulation showed the resulting solutions exploit regions of favorable tailwinds in order to reduce battery consumption [15]. A dynamically feasible trajectory was obtained through the solution of an optimal control problem using pseudospectral optimal control software by Grymin [16]. Tang focused on the problem of minimum time trajectory planning by pseudospectral method for helicopter UAVs [17]. Adaptive pseudospectral was used to gain the offline trajectory of formation generation for quadcopters by Zhang [18]. It can be seen from the above literature, pseudospectral method has a great performance for trajectory optimization of a single UAV. However, the collision avoidance constraints between UAVs for the formation generation problem were transformed into the problem that large number of path constraints will increase the computation time greatly.

It should be noted that suitable initial guess closely related to the computation time. In order to reduce the computation time, some optimization methods were proposed to obtain a better path as the initial guess. Yu proposed a modified wolf swarm search algorithm combined with genetic algorithm to calculate the UAV path [19]. Differential evolution algorithm was used to provide a better initial guess for space maneuver vehicle trajectory planning by Tsourdos [20], so the collision avoidance for the formation problem is not exist. RRT method was adopted to achieve real-time flight-path planning for multirotor aerial vehicles [21]. A new hybrid collision avoidance method along with a modified path following approach was proposed to reduce the computational efforts and satisfied the performance of collision avoidance [22]. A new ant colony optimization approach to path planning in dynamic environments to achieve the obstacle avoidance, however the computational time values vary from about ten to 60 seconds, which is not suitable for the helicopters [23]. A hybridization of an improved particle swarm optimization (IPSO) and an improved gravitational search algorithm (IGSA) was proposed for multi-robot path planning, which has a better performance for the different meta-heuristic algorithms such as IGSA, IPSO through the simulation, however could not satisfy the strong real-time requirements [24]. An improved RRT algorithm was proposed to gain the near optimal path that taking into account the dynamic constraints [25].

Along with the safety trajectory, a robust finite-time control strategy aiming at tracking the safety trajectory was indispensable to achieve the formation generation. Most of the trajectory tracking of unmanned helicopter adopted linear control methods. A H_∞ attitude tracking controller was designed for the attitude inner loop of unmanned helicopter and an position outer loop tracking control algorithm was designed via the dynamic inverse approach to achieve tracking control [26]. The feedback linearization and extended high gain observation methods were applied to propose a formation controller for unmanned helicopters system [27]. However, it is known that linear model can only be used for flight control around reference equilibrium points which is not suitable for the nonlinear model. It is reasonable and effective to propose a nonlinear controller suitable for the nonlinear model. Based on nonlinear control method, a smooth outer loop controller was proposed to achieve the asymptotic tracking for helicopter by Karimoddini [28]. The distributed cooperative controller based on linear sliding mode controller was designed for underactuated quadrotors when the reference signal was not available to all the vehicles by Ghommam [29]. A novel robust terminal sliding mode control algorithm was proposed to achieve the robust control avoiding the chattering phenomenon for a quadrotor UAV [30]. In recent years, finite-time theories were widely used in the UAV, spacecraft and Reusable Launch Vehicle (RLV) control [31]– [36]. A controller design method using nonsingular terminal sliding mode surface and extended state observers (ESOs) was proposed to solve the finite-time convergence problem of system states in course of the transition flight control for a small tilt rotor UAV [37]. Finite-time disturbance observer-based controllers were designed for the quadrotor model using homogeneity theory [38].

In the past few years, many collision avoidance algorithms have been designed of the formation generation process for spacecraft and UAVs. A hybrid particle swarm optimization and genetic algorithm was proposed to solve formation reconfiguration problem by Duan [39]. A semianalytic approach was developed to achieve fuel-minimized, collision-free path generation for satellites formation [40]. Potential energy function method was the most common method for formation collision avoidance control, which is more suitable for large-scale UAVs formation. An optimized artificial potential field (APF) algorithm with distance factor and jump strategy was proposed for multi-UAV operation in 3D dynamic space [41]. The controller based on the decentralized navigation function was used to achieve collision avoidance in multi-agent systems [42]. The potential function based-RRT*

that incorporates the artificial potential field algorithm was proposed to improve a more efficient memory utilization and accelerated convergence rate [43].

Motivated by the aforementioned discussion, a novel safe formation generation scheme is developed for unmanned helicopters in the presence of external disturbance and model uncertainty. In this paper, the main contributions of the work are twofold. Firstly, the safe trajectory is obtained by the pseudospectral method and SQP method, in which RRT method is proposed to obtain a better initial guess. Secondly, a new finite-time tracking controller based on sliding mode method combined with the potential function method is designed to achieve the high precision control performance.

The rest of the paper is organized as follows: the model description, path constraints and control objective in the research are formulated in Sec. II. The novel formation generation scheme are given in Sec. III. The simulation results are provided in Sec. IV. Finally, conclusions remarks are summarized in Sec. V.

II. PROBLEM FORMULATION

In this paper, the problem of unmanned helicopters formation generation is investigated. The mathematical model, constraints and control objective are given as follows.

A. MATHEMATICAL MODEL

Ignoring the lift generated by lateral and longitudinal periodic variable angles in the x, y directions and coupling among lateral, longitudinal periodic variable angles and tail rotor, the equations of six-degrees-of-freedom rigid body model for helicopters can be described by the following equations [44]

$$\begin{aligned}
\dot{\mathbf{P}}_i &= \mathbf{V}_i \\
\dot{\mathbf{V}}_i &= g\mathbf{e}_3 + \mathbf{R}_i\mathbf{e}_3(-g + Z_w^i w_i) + \mathbf{U}_{1i} + \mathbf{d}_{Vi} \\
\dot{\mathbf{\Theta}}_i &= \mathbf{\Pi}_i(\mathbf{\Theta}_i)\mathbf{\Omega}_i \\
\dot{\mathbf{\Omega}}_i &= -\mathbf{J}_i^{-1}\mathbf{S}(\mathbf{\Omega}_i)\mathbf{J}_i\mathbf{\Omega}_i + \mathbf{A}_i\mathbf{\Omega}_i + \mathbf{e}_3 N_{col}^i \delta_{col}^i + \mathbf{B}_i\mathbf{U}_{2i} + \mathbf{d}_{\Omega i}
\end{aligned} \tag{1}$$

where $\mathbf{P}_i = [x_i, y_i, z_i]^T$, $\mathbf{V}_i = [u_i, v_i, w_i]^T$ are the position and velocity vector of the ith helicopter in the inertial frame, g is the acceleration due to gravity, $\mathbf{e}_3 = [0, 0, 1]^T$, $\mathbf{R}_i$ is rotation matrix from body coordinate system to inertial frame, $\mathbf{U}_{1i} = [U_{1xi}, U_{2yi}, U_{3zi}]^T = \mathbf{R}_i\mathbf{e}_3 Z_{col}^i \delta_{col}^i$ is the intermediate control vector for outer loop system, δ_{col}^i is main rotor collective pitch angle, Z_{col}^i, N_{col}^i are the known gains, $\mathbf{d}_{Vi}, \mathbf{d}_{\Omega i}$ are the integrated interference term caused by model uncertainty and external disturbances, $\mathbf{\Theta}_i = [\phi_i, \theta_i, \psi_i]^T$ is the Euler angle vector in the inertial frame, $\mathbf{\Omega}_i = [p_i, q_i, r_i]^T$ is the angular rate vector in the body frame, $\mathbf{\Pi}_i(\mathbf{\Theta}_i)$ is the attitude rotation matrix, $\mathbf{J}_i$ is the diagonal inertia matrix, $\mathbf{S}(\mathbf{\Omega}_i)$ is a skew-symmetric matrix, $\mathbf{A}_i, \mathbf{B}_i$ are the system matrix of control, $U_{2i} = [\delta_{lon}^i, \delta_{lat}^i, \delta_{ped}^i]^T$ is the attitude control vector. The rotation matrix $\mathbf{R}_i$ is given as follows

$$\mathbf{R}_i = \begin{bmatrix} C_{\theta i}C_{\psi i} & S_{\phi i}S_{\theta i}C_{\psi i} - C_{\phi i}S_{\psi i} & C_{\phi i}S_{\theta i}C_{\psi i} + S_{\phi i}S_{\psi i} \\ C_{\theta i}S_{\psi i} & S_{\phi i}S_{\theta i}S_{\psi i} + C_{\phi i}S_{\psi i} & C_{\phi i}S_{\theta i}S_{\psi i} - S_{\phi i}C_{\psi i} \\ -S_{\theta i} & S_{\phi i}C_{\theta i} & C_{\phi i}C_{\theta i} \end{bmatrix} \tag{2}$$

where C is $\cos(\cdot)$, S is $\sin(\cdot)$.

Ignoring the external disturbances, the particle model using in the part of trajectory optimization for helicopters is given as follows

$$\begin{aligned}
\dot{\mathbf{P}}_i &= \mathbf{V}_i \\
\dot{\mathbf{V}}_i &= g\mathbf{e}_3 + \mathbf{R}_i\mathbf{e}_3(-g + Z_w^i w_i + Z_{col}^i \delta_{col}^i)
\end{aligned} \tag{3}$$

where $T_{mi} = -g + Z_w^i w_i + Z_{col}^i \delta_{col}^i$ is the main rotor thrust for the ith helicopters, the formula(3) can be shown as follows

$$\begin{aligned}
\dot{\mathbf{P}}_i &= \mathbf{V}_i \\
\dot{\mathbf{V}}_i &= g\mathbf{e}_3 + \mathbf{R}_i\mathbf{e}_3 T_{mi}
\end{aligned} \tag{4}$$

B. CONSTRAINTS

The path constraints during the process of formation generation for unmanned helicopters include state variables, boundary value and collision avoidance constraints.

Taking small unmanned helicopter as controlled object, the state variables need to satisfy the following constraints:

$$\begin{aligned}
&|x_i| \le 300m; \quad |y_i| \le 300m; \quad 0 \le z_i \le 300m \\
&|u_i| \le 10m/s; \quad |v_i| \le 10m/s; \quad |w_i| \le 10m/s \\
&|\phi_i| \le 25^{\circ}; \quad |\theta_i| \le 25^{\circ}; \quad |\psi_i| \le 25^{\circ}
\end{aligned} \tag{5}$$

The boundary value constraints contain the state and control variables in the initial and final time points. Considering the helicopters take off from three areas, the position variables in the initial and final time points is given as follows:

$$\begin{aligned}
\mathbf{P}_1\,(initial) &= [0, 240, 0]^T\, m;\ \mathbf{P}_1\,(final) = [240, 260, 0]^T\, m \\
\mathbf{P}_2\,(initial) &= [0, 250, 0]^T\, m;\ \mathbf{P}_2\,(final) = [250, 270, 0]^T\, m \\
\mathbf{P}_3\,(initial) &= [10, 250, 0]^T\, m;\ \mathbf{P}_3\,(final) = [260, 260, 0]^T\, m \\
\mathbf{P}_4\,(initial) &= [250, 10, 0]^T\, m;\ \mathbf{P}_4\,(final) = [270, 250, 0]^T\, m \\
\mathbf{P}_5\,(initial) &= [240, 10, 0]^T\, m;\ \mathbf{P}_5\,(final) = [260, 250, 0]^T\, m \\
\mathbf{P}_6\,(initial) &= [250, 0, 0]^T\, m;\ \mathbf{P}_6\,(final) = [260, 240, 0]^T\, m \\
\mathbf{P}_7\,(initial) &= [240, 0, 0]^T\, m;\ \mathbf{P}_7\,(final) = [250, 230, 0]^T\, m \\
\mathbf{P}_8\,(initial) &= [0, 0, 0]^T\, m;\ \mathbf{P}_8\,(final) = [240, 240, 0]^T\, m \\
\mathbf{P}_9\,(initial) &= [10, 0, 0]^T\, m;\ \mathbf{P}_9\,(final) = [240, 250, 0]^T\, m \\
\mathbf{P}_{10}\,(initial) &= [0, 10, 0]^T\, m;\ \mathbf{P}_{10}\,(final) = [230, 250, 0]^T\, m
\end{aligned} \tag{6}$$

In the initial and final time points, the velocity vector for helicopters need to be zero, which is given as follows:

$$\mathbf{V}_i\,(initial) = \mathbf{V}_i\,(final) = [0, 0, 0]^T\, m/s, \quad i = 1, 2, \cdots, 10 \tag{7}$$

In the initial time points, the Euler angle vector need to be zero. Considering the range of Euler angle vector is relatively small, the Euler angle vector in the final time can be free, which is given as follows:

$$\begin{cases} \mathbf{\Theta}_i\,(initial) = [0, 0, 0]^T \\ \mathbf{\Theta}_i\,(final) = [free, free, free]^T, \quad i = 1, 2, \cdots, 10 \end{cases} \tag{8}$$

In addition, the collision avoidance constraints between UAVs are given in the form of linear constraints as followsčž

$$\begin{cases} |x_i - x_j| \geq 5m \\ |y_i - y_j| \geq 5m, \quad i \neq j, \\ |z_i - z_j| \geq 5m \end{cases} \tag{9}$$

C. CONTROL OBJECTIVE

In this paper, the formation generation process of unmanned helicopters through trajectory optimization and control is presented. In the part of trajectory optimization, the main objective is to design optimal trajectories for the unmanned helicopters formation which aim at minimize the flying time:

$$\min J = t_{f(1)} = t_{f(2)} = \cdots = t_{f(n)} = t_f \tag{10}$$

where $t_{f(i)}$ is the flying time of the ith unmanned helicopters.

In the part of control, a finite-time controller is designed to achieve the high precision robust tracking control for the unmanned helicopters formation.

III. TRAJECTORY OPTIMIZATION AND CONTROL DESIGN

As shown in FIGURE 1, the structure of trajectory optimization and control are given as follows. In the part of trajectory optimization, the safe path for the unmanned helicopters formation is given through RRT algorithm as initial guess. The trajectory optimization can be discretized to a NLP problem and solved by the SQP method. In the part of control, the nonlinear model for unmanned helicopter is established. The finite-time position outer and attitude inner controller based on the terminal sliding mode are proposed to achieve the high-precision tracking control and the system stability proof is finished by Lyapunov function combined with the multi-scale principle.

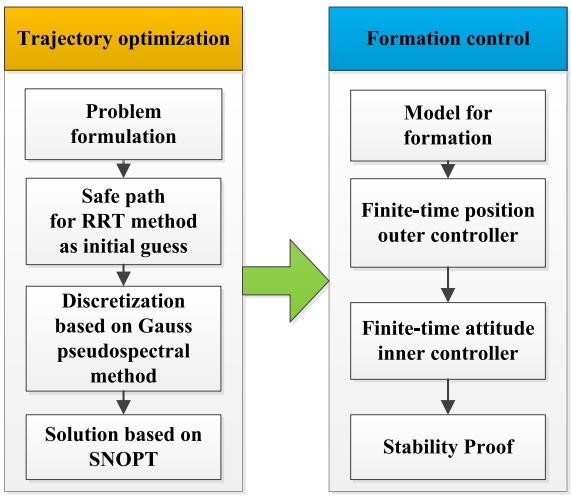

FIGURE 1. The structure of the optimization and control.

A. TRAJECTORY OPTIMIZATION

Firstly, RRT method is applied to acquire safe paths as a better initial guess to increase the convergence speed. Then, the Gauss pseudospectral method is used to convert the optimal control problem into a NLP problem and solved by SQP method to gain the optimal trajectory.

1) GAUSS PSEUDOSPECTRAL METHOD

A new discrete strategy is proposed by pseudospectral method. The pseudospectral method mainly includes three methods: Gauss, Legendre and Radau pseudospectral method. Among them, Gauss pseudospectral method has the most complete proof of first-order optimality and the highest precision which is applied in the paper.

The detailed discretization steps are given as follows:

Firstly, the root of Legendre polynomials located in the time domain $\tau \in [-1, 1]$ is chosen as the collocation point, which is different from the time domain of actual trajectory. Therefore, the time interval t of trajectory for unmanned helicopters formation is transformed into the time interval τ of the Gauss pseudospectral method by time domain transformation:

$$t \in [t_0, t_f] \to \tau \in [-1, 1], \quad \tau = \frac{2t}{t_f - t_0} - \frac{t_f + t_0}{t_f - t_0} \tag{11}$$

where t_0 is the initial time of trajectory optimization, t_f is the final time of trajectory optimization, τ is the time interval satisfying the requirement of Gauss pseudospectral method.

Secondly, K is chosen as the number of discrete points, the collocation points is K-order Legendre-Gauss (LG) points, i.e. the root of K-order Legendre polynomials, where Legendre polynomial $P_K(\tau)$ is given as follows

$$P_K(\tau) = \frac{1}{2^K K!} \frac{d^K}{d\tau^K} \left[\left(\tau^2 - 1 \right)^K \right] \tag{12}$$

Thirdly, continuous state variable discretized by Lagrange interpolation polynomials based on discrete points is given as follows

$$\begin{aligned} \mathbf{x}(\tau) &\approx \mathbf{X}(\tau) = \sum_{i=0}^{K} L_i(\tau) \mathbf{X}(\tau_i) \\ L_i(\tau) &= \prod_{j=0, j \neq i}^{N} \frac{\tau - \tau_j}{\tau_i - \tau_j} = \frac{g(\tau)}{(\tau - \tau_i)\dot{g}(\tau)} \end{aligned} \tag{13}$$

where $g(\tau) = (1 + \tau) P_N(\tau)$, $\mathbf{X}(\tau_i)$ is the τ_ith discrete point of state variable.

Similarly, the discretization of control variable is expressed as follows

$$\mathbf{u}(\tau) \approx \mathbf{U}(\tau) = \sum_{i=1}^{K} L_i(\tau) \mathbf{U}(\tau_i) \tag{14}$$

where $\mathbf{U}(\tau_i)$ is the τ_ith discrete point of control variable.

Fourthly, the terminal time point is not contained in the discrete points of Gauss pseudospectral method, the state variable need to be obtained by integration as follows

$$\mathbf{X}(\tau_f) = \mathbf{X}(\tau_0) + \int_{-1}^{1} f\left(\mathbf{X}(\tau), \mathbf{U}(\tau), \tau\right) d\tau \tag{15}$$

The terminal state $\mathbf{X}(\tau_f)$ is discretized by integrating the Lagrange interpolation polynomials as follows

$$\mathbf{X}(\tau_f) = \mathbf{X}(\tau_0) + \frac{t_f - t_0}{2} \sum w_k f\left(\mathbf{X}(\tau_k), \mathbf{U}(\tau_k), \tau, t_0, t_f\right)$$
$$w_k = \int_{-1}^{1} L_i(\tau) d\tau = \frac{2}{(1-\tau_i^2)\left[\dot{P}_K(\tau_i)\right]^2} \tag{16}$$

where w_k is the Gaussian weight.

Fifthly, the discretization approximation of the derivative parts obtained by deriving the Lagrange interpolation polynomial is given as follows

$$\dot{\mathbf{x}}(\tau_k) \approx \dot{\mathbf{X}}(\tau_k) = \sum_{i=0}^{K} \dot{L}_i(\tau_k)\mathbf{X}(\tau_i) = \sum_{i=0}^{k} D_{ki}\mathbf{X}(\tau_i)$$
$$D_{ki} = \begin{cases} \dfrac{(1+\tau_k)\dot{P}_K(\tau_k) + P_K(\tau_k)}{(\tau_k - \tau_i)\left[(1+\tau_i)\dot{P}_K(\tau_i) + P_K(\tau_i)\right]}, & i \neq k \\ \dfrac{(1+\tau_i)\ddot{P}_K(\tau_i) + 2\dot{P}_K(\tau_i)}{2\left[(1+\tau_i)\dot{P}_K(\tau_i) + P_K(\tau_i)\right]}, & i = k \end{cases} \tag{17}$$

The whole discretization process is presented from (11) to (17) and the optimal control problem is finally converted to a NLP problem.

2) INITIAL GUESS

For the rapidity and safety requirements of unmanned helicopters formation generation, a better initial guess is provided by RRT algorithm to reduce the computation time of trajectory optimization.

RRT method is established by incremental methods with a tree-shaped data storage structure which can rapidly reducing the distance between randomly selected points and expected points. As shown in FIGURE 2, node expansion diagram of RRT method is given.

The specific solution steps are given as follows:

Step1 (Random Path Point Selection): The target position q_{goal} of formation generation is selected as the random path point q_{rand} by probability p_g or a random path point in the task space is selected as the random path point q_{rand} by probability $1 - p_g$.

Step2 (Adjacent Path Point Selection): From current leaf nodes of the random tree, the node nearest to the random path point q_{rand} is selected as the adjacent node q_{near}.

Step3 (New Path Point Selection): The new path point q_{new} is obtained by extending one step distance from the direction of q_{near} to the direction of q_{rand}. The collision confliction is determined during the extension process. If there is no conflict between the new path point q_{new} and path point for the other unmanned helicopters, q_{new} is accepted and added as a node of the random tree; if the confliction maybe occurs with the threat area, the new node is discarded and the random node q_{rand} is selected again until the security requirements are met.

Step4 (Search Stop Judgment): Judging whether the new node reach the neighborhood of the target node. If this condition is satisfied, the random search process should be stopped; if not, back to the Step2.

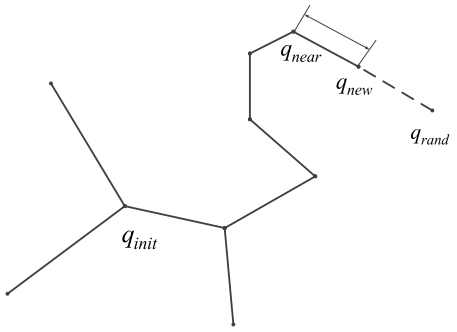

FIGURE 2. Node Expansion Diagram of RRT method.

3) COLLISION AVOIDANCE STRATEGY

The unmanned helicopters in formation calculate their own safety path points in turn. Considering the requirement of the fast formation generation and the same search step size between the unmanned helicopters, when judging the collision confliction conditions in the kth iteration for the ith unmanned helicopter, the path points from the $k-1$th to the $k+1$th iteration for the other helicopters are considered. So the safe flying for the unmanned helicopters can be achieved when the collision avoidance conditions are satisfied.

The trajectory optimization is carried out using SNOPT solver based on SQP method. SNOPT is a software package for solving large-scale optimization problems which is effective for NLP problems.

B. CONTROLLER DESIGN

When optimal trajectory is obtained as the desired command, the finite-time tracking controller for the unmanned helicopter formation is designed to realize the high-precision tracking.

Firstly, a terminal sliding mode virtual speed controller is designed to ensure accurate tracking for the position reference command. Further, the terminal outer loop controller is designed to realize the tracking of the virtual speed. In the part of attitude inner loop, the reference command of the attitude is obtained by attitude calculation. Based on the second-order sliding mode control method, the inner loop controller is designed to ensure the stable tracking control of the inner loop attitude to the reference command. The stability of outer and inner loop system are proved by combining the existing multi-time scale criteria. The specific design process is given as follows:

Several assumptions and lemmas are given to prepare for the stability proofs.

Assumption 1: It is assumed that the outer loop disturbances $\mathbf{d}_{Vi}$ are bounded, and there exist known positive constant k_{Vi} such that the conditions $\|\mathbf{d}_{Vi}\| \leq k_{Vi}, i = 1, ..., n$ hold.

Assumption 2: It is assumed that the inner loop disturbances $\mathbf{d}_{\Omega i}$ and its derivatives are bounded, and there exist

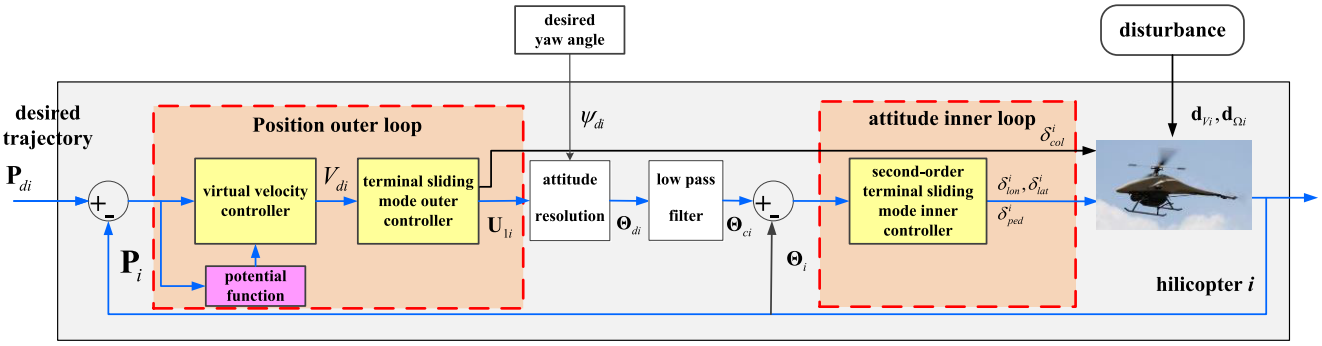

FIGURE 3. Structure of Unmanned Helicopter Trajectory Tracking Controller.

positive constants, $k_{\Omega i}$ and $\tilde{k}_{\Omega i}$, such that the conditions $\|\mathbf{d}_{\Omega i}\| \le k_{\Omega i}$ and $\left\|\dot{\mathbf{d}}_{\Omega i}\right\| \le \tilde{k}_{\Omega i}$ hold.

Assumption 3 [45], [46]: The derivative of desired trajectory is bounded.

Lemma 1 [47]: For the following system

$$\begin{aligned} \dot{\boldsymbol{\sigma}} &= -k_1 \frac{\boldsymbol{\sigma}}{\|\boldsymbol{\sigma}\|^{\frac{1}{2}}} - k_2 \boldsymbol{\sigma} + \boldsymbol{\xi} \\ \dot{\boldsymbol{\xi}} &= -k_3 \frac{\boldsymbol{\sigma}}{\|\boldsymbol{\sigma}\|} - k_4 \boldsymbol{\sigma} + \Delta(t) \end{aligned} \tag{18}$$

where $\boldsymbol{\sigma} \in R^n$ is system state, $\|\Delta(t)\| \le \delta$, δ is a known scalar bound, there exists a range of values for the gains k_1, k_2, k_3, k_4, such that the variables $\boldsymbol{\sigma}$ and $\dot{\boldsymbol{\sigma}}$ are forced to zero in finite time and remain zero for all subsequent time.

When the trajectory of each unmanned helicopter is determined, the design of trajectory controller becomes the key to achieve the formation generation. A finite-time position and a finite-time attitude controller are designed.

1) POSITION TRACKING CONTROLLER DESIGN

Position tracking error vector $\bar{\mathbf{e}}_{Pi}$ is defined as follows

$$\bar{\mathbf{e}}_{Pi} = \mathbf{P}_{di} - \mathbf{P}_i \tag{19}$$

where $\mathbf{P}_{di}$ is the desired trajectory for ith unmanned helicopter, $\mathbf{P}_i$ is the position of ith unmanned helicopter.

Define assist tracking error vector $\mathbf{e}_{Pi}$

$$\mathbf{e}_{Pi} = \mathbf{P}_{di} - \mathbf{P}_i - \sum_{i,j=1,i\neq j}^{n} \frac{\partial \gamma_{ij}^a}{\partial \mathbf{P}_i} \tag{20}$$

where γ_{ij}^a is the potential energy function to describe the collisions between unmanned helicopters which is given as follows

$$\gamma_{ij}^a = \begin{cases} \eta_j \varepsilon_a^{(\rho_a - \|\mathbf{P}_i - \mathbf{P}_j\|)/(\rho_a - r_a)}, & if \ \left\|\mathbf{P}_i - \mathbf{P}_j\right\| < r_a \\ 0, & \text{otherwise} \end{cases} \tag{21}$$

where $\eta_j > 0, 0 < \varepsilon_a < 1, 0 < \rho_a < r_a$,$r_a$ is the safe flight radius of unmanned helicopter.

The virtual velocity controller $\mathbf{V}_{di}$ is designed by

$$\mathbf{V}_{di} = k_{1Vi} sig^{\frac{1}{2}}(\mathbf{e}_{Pi}) + k_{2Vi} sign(\mathbf{e}_{Pi}) + \dot{\mathbf{P}}_{di} \tag{22}$$

where $sig^{\frac{1}{2}}(\mathbf{e}_{Pi}) = [|\mathbf{e}_{Pi1}|^{\frac{1}{2}} sgn(\mathbf{e}_{Pi1}), |\mathbf{e}_{Pi2}|^{\frac{1}{2}} sgn(\mathbf{e}_{Pi2}), |\mathbf{e}_{Pi3}|^{\frac{1}{2}} sgn(\mathbf{e}_{Pi3})]$, $k_{1Vi} > 0$, $k_{2Vi} > 0$. The outer controller based on the terminal sliding mode is given by

$$\begin{aligned} \mathbf{U}_{1i} = -g\mathbf{e}_3 - \mathbf{R}_i \mathbf{e}_3 (-g + Z_w^i w_i) + k_{3Vi} sig(\mathbf{e}_{Vi})^{\frac{1}{2}} \\ + k_{4Vi} sign(\mathbf{e}_{Vi}) + \dot{V}_{di} \end{aligned} \tag{23}$$

Then the collective pitch of main rotor can be described as follows

$$\delta_{col}^i = \sqrt{U_{1i}^T U_{1i}} / Z_{col}^i \tag{24}$$

Finite-Time Integral Filters:

It is difficult to obtaining the derivative of the virtual controller V_{di}, because this signal may not be practically differentiable. Based on this, we use the finite-time integral filter designed in our previous paper [41].

The finite-time integral filter of virtual and its derivative are designed as

$$\begin{aligned} \dot{\xi}_{1i} &= -\frac{\xi_{1i} - V_{di}}{\tau_{1i}} - \frac{l_{1i}(\xi_{1i} - V_{di})}{\|\xi_{1i} - V_{di}\|^{\frac{1}{2}} + m_{1i}} \\ \dot{\xi}_{2i} &= -\frac{\xi_{2i} - \dot{\xi}_{1i}}{\tau_{2i}} - \frac{l_{2i}(\xi_{2i} - \dot{\xi}_{1i})}{\left\|\xi_{2i} - \dot{\xi}_{1i}\right\|^{\frac{1}{2}} + m_{2i}} \end{aligned} \tag{25}$$

Then, the output of integral filters replaces the derivative of the virtual controller.

2) ATTITUDE RESOLUTION

Because the trajectory tracking control cannot be realized by the attitude control variables, the desired attitude angle must be obtained through the attitude resolution.

Defining the desired attitude angle $\boldsymbol{\Theta}_{di} = [\phi_{di}, \theta_{di}, \psi_d]^T$, the desired yaw angle ψ_{di} of unmanned helicopter is given by the desired trajectory. Combined with the relationship $\mathbf{U}_{1i} = \mathbf{R}_i \mathbf{e}_3 Z_{col}^i \delta_{col}^i$ among rotation matrix $\mathbf{R}_i$, main rotor pitch angle δ_{col}^i and outer loop controller $\mathbf{U}_{1i}$ and the property of rotating matrix $\mathbf{R}_i^T \mathbf{R}_i = \mathbf{I} \in R^{3\times 3}$, the desired roll angle ϕ_{di} and pitch angle θ_{di} are given as follows

$$\phi_{di} = \arcsin\left(\frac{S_{\psi i} U_{1xi} - C_{\psi i} U_{1yi}}{\sqrt{\left(U_{1xi}^2 + U_{1yi}^2 + U_{1zi}^2\right)}} \right)$$

$$\theta_{di} = \arctan\left(\frac{C_{\psi i}U_{1xi} + S_{\psi i}U_{1yi}}{U_{1zi}}\right) \tag{26}$$

In the following, the second derivative of the attitude controller is estimated in the same way. The finite-time integral filter of desired attitude angle, its derivative, and its second derivative are designed as

$$\begin{aligned}
\dot{\Theta}_{1ci} &= -\frac{\Theta_{1ci} - \Theta_{di}}{\tau_{3i}} - \frac{l_{3i}(\Theta_{1ci} - \Theta_{di})}{\|\Theta_{1ci} - \Theta_{di}\|^{\frac{1}{2}} + m_{3i}} \\
\dot{\Theta}_{2ci} &= -\frac{\Theta_{2ci} - \dot{\Theta}_{1ci}}{\tau_{4i}} - \frac{l_{4i}(\Theta_{2ci} - \dot{\Theta}_{1ci})}{\left\|\Theta_{2ci} - \dot{\Theta}_{1ci}\right\|^{\frac{1}{2}} + m_{4i}} \\
\dot{\Theta}_{3ci} &= -\frac{\Theta_{3ci} - \dot{\Theta}_{2ci}}{\tau_{5i}} - \frac{l_{5i}(\Theta_{3ci} - \dot{\Theta}_{2ci})}{\left\|\Theta_{3ci} - \dot{\Theta}_{2ci}\right\|^{\frac{1}{2}} + m_{5i}}
\end{aligned} \tag{27}$$

3) ATTITUDE TRACKING CONTROLLER DESIGN

Define attitude tracking error vector $\mathbf{e}_{\Theta i} = \mathbf{\Theta}_{di} - \mathbf{\Theta}_i$. The terminal sliding mode surface $\mathbf{s}_{\Theta i}$ is designed as follows

$$\mathbf{s}_{\Theta i} = \dot{\mathbf{e}}_{\Theta i} + \beta_{2i} sig^{\frac{1}{2}}(\mathbf{e}_{\Theta i}) \tag{28}$$

where $\beta_{2i} > 0$. If $\mathbf{s}_{\Theta i} = 0$ holds, the attitude angle tracking error $\mathbf{e}_{\Theta i}$ and its derivatives can converge to zero in finite time considering the characteristics of the terminal sliding mode, which means the output of the system $\mathbf{\Theta}_i$ can track the desired output $\mathbf{\Theta}_{di}$.

The $\dot{\mathbf{s}}_{\Theta i}$ can be calculated by

$$\begin{aligned}
\dot{\mathbf{s}}_{\Theta i} &= \ddot{\mathbf{e}}_{\Theta i} + \frac{1}{2}\beta diag(|\mathbf{e}_{\Theta i}|^{-\frac{1}{2}})\dot{\mathbf{e}}_{\Theta i} \\
&= \ddot{\mathbf{\Theta}}_{di} - \dot{\mathbf{\Pi}}(\mathbf{\Theta}_i)\mathbf{\Omega}_i + \frac{1}{2}\beta diag(|\mathbf{e}_{\Theta i}|^{-\frac{1}{2}})\dot{\mathbf{e}}_{\Theta i} - \mathbf{\Pi}(\mathbf{\Theta}_i) \\
&\quad \cdot \left(-\mathbf{J}_i^{-1}\mathbf{S}(\mathbf{\Omega}_i)\mathbf{J}_i\mathbf{\Omega}_i + \mathbf{A}_i\mathbf{\Omega}_i + \mathbf{e}_3 N_{col}^i \delta_{col}^i + \mathbf{B}_i\mathbf{U}_{2i} + \mathbf{d}_{\Omega i}\right)
\end{aligned} \tag{29}$$

Then, design the attitude tracking controller $\mathbf{U}_{2i}$

$$\begin{aligned}
\mathbf{U}_{2i} = \mathbf{B}_i^{-1}\mathbf{\Pi}(\mathbf{\Theta}_i)^{-1}[&\Theta_{3ci} - \dot{\mathbf{\Pi}}(\mathbf{\Theta}_i)\mathbf{\Omega}_i + \frac{1}{2}\beta diag(|\mathbf{e}_{\Theta i}|^{-\frac{1}{2}})\dot{\mathbf{e}}_{\Theta i} \\
&- \mathbf{\Pi}(\mathbf{\Theta}_i)(-\mathbf{J}_i^{-1}\mathbf{S}(\mathbf{\Omega}_i)\mathbf{J}_i\mathbf{\Omega}_i + \mathbf{A}_i\mathbf{\Omega}_i + \mathbf{e}_3 N_{col}^i \delta_{col}^i) \\
&+ k_{1\Theta i}\frac{\mathbf{s}_{\Theta i}}{||\mathbf{s}_{\Theta i}||^{\frac{1}{2}}} + k_{2\Theta i}\mathbf{s}_{\Theta i} + \int\left(k_{3\Theta i}\frac{\mathbf{s}_{\Theta i}}{||\mathbf{s}_{\Theta i}||} + k_{4\Theta i}\mathbf{s}_{\Theta i}\right)dt]
\end{aligned} \tag{30}$$

where $k_{1\Theta i} > 0, k_{2\Theta i} > 0, k_{3\Theta i} > 0, k_{4\Theta i} > 0$.

4) STABILITY PROOF FOR THE POSITION SYSTEM

Theorem 1: Consider the UAV system (1) satisfying Assumption 1, if the outer controller is designed as (22)-(23), and choose $k_{1Vi} > 0, k_{2Vi} > \left\|\dot{\mathbf{P}}_{di}\right\|, k_{3Vi} > 0, k_{4Vi} > \|\mathbf{d}_{Vi}\|$, then the trajectory tracking errors $\mathbf{e}_{Pi}$ will converge to zero in finite-time.

Proof: Trajectory tracking error vector $\mathbf{e}_{Vi}$ is defined as follows

$$\mathbf{e}_{Vi} = \mathbf{V}_{di} - \mathbf{V}_i \tag{31}$$

where $\mathbf{V}_i$ is the velocity of ith unmanned helicopter.

Choose the following candidate Lyapunov function Φ_1 as follows

$$\Phi_1 = \frac{1}{2}\sum_{i=1}^{n}\mathbf{e}_{Vi}^T\mathbf{e}_{Vi} \tag{32}$$

The derivative of Φ_1 is

$$\begin{aligned}
\dot{\Phi}_1 &= \sum_{i=1}^{n}\mathbf{e}_{Vi}^T\dot{\mathbf{e}}_{Vi} \\
&= \sum_{i=1}^{n}\mathbf{e}_{Vi}^T\left(\dot{\mathbf{V}}_{di} - g\mathbf{e}_3 - \mathbf{R}_i\mathbf{e}_3(-g + Z_w^i w_i) - \mathbf{U}_{1i} - \mathbf{d}_{Vi}\right) \\
&\le -k_{3Vi}\Phi_1^{\frac{3}{4}} - k_{4Vi}\sum_{i=1}^{n}\|\mathbf{e}_{Vi}\| + \sum_{i=1}^{n}\|\mathbf{e}_{Vi}\|\left\|\mathbf{d}_{Vi} + \dot{\mathbf{V}}_{di} - \xi_{2i}\right\| \\
&= -k_{3Vi}\Phi_1^{\frac{3}{4}} - k_{4Vi}\sum_{i=1}^{n}\|\mathbf{e}_{Vi}\| \\
&\quad + \sum_{i=1}^{n}\|\mathbf{e}_{Vi}\|\left\|\mathbf{d}_{Vi} + \dot{\mathbf{V}}_{di} - \xi_{1i} + \xi_{1i} - \xi_{2i}\right\|
\end{aligned} \tag{33}$$

According to Assumption 1, the disturbances $\|\mathbf{d}_{Vi}\|$ have a bound. Let $k_{4Vi} > \left\|\mathbf{d}_{Vi} + \dot{\mathbf{V}}_{di} - \xi_{1i} + \xi_{1i} - \xi_{2i}\right\|$, where $\dot{\mathbf{V}}_{di} - \xi_{1i} + \xi_{1i} - \xi_{2i}$ is the sum filter errors, then $\dot{\Phi}_1 \le -k_{3Vi}\Phi_1^{\frac{3}{4}}$. The velocity tracking error of ith unmanned helicopter can converge to zero in finite-time. The sum filter errors $\dot{\mathbf{V}}_{di} - \xi_{1i} + \xi_{1i} - \xi_{2i}$ can converge to zero in finite-time according to [41].

Then, it is proved that the trajectory tracking error $\mathbf{e}_{Pi}$ of ith unmanned helicopter will not diverge before the virtual velocity is traced at finite time. Consider the following candidate Lyapunov function

$$\Phi_2 = \frac{1}{2}\sum_{i=1,j=1,i\neq j}^{n}\left(\bar{\mathbf{e}}_{Pi}^T\bar{\mathbf{e}}_{Pi} + \gamma_{ij}^a\right) + \frac{1}{2}\sum_{i=1}^{n}\mathbf{e}_{Vi}^T\mathbf{e}_{Vi} \tag{34}$$

The derivative of Φ_2 is taking as follows

$$\begin{aligned}
\dot{\Phi}_2 &= \sum_{i=1}^{n}\left(\frac{\partial\bar{\mathbf{e}}_{Pi}^T\bar{\mathbf{e}}_{Pi}}{\partial\mathbf{P}_i} + \frac{\partial\gamma_{ij}^a}{\partial\mathbf{P}_i}\right)^T\dot{\mathbf{P}}_i + \sum_{i=1}^{n}\mathbf{e}_{Vi}^T\left(\dot{\mathbf{V}}_{di} - \dot{\mathbf{V}}_i\right) \\
&= -\sum_{i=1}^{n}\left(\bar{\mathbf{e}}_{Pi} - \frac{\partial\boldsymbol{\gamma}_{ij}^a}{\partial\mathbf{P}_i}\right)^T(\mathbf{V}_{di} - \mathbf{e}_{Vi}) \\
&\quad + \sum_{i=1}^{n}e_{Vi}^T\left(\dot{\mathbf{V}}_d - g\mathbf{e}_3 - \mathbf{R}_i\mathbf{e}_3(-g + Z_w^i w_i) - \mathbf{U}_{1i} - \mathbf{d}_{Vi}\right)
\end{aligned} \tag{35}$$

Further, we derive

$$\begin{aligned}
\dot{\Phi}_2 = -\sum_{i=1}^{n}(\bar{\mathbf{e}}_{Pi} - \frac{\partial\gamma_{ij}^a}{\partial\mathbf{P}_i})^T[k_{1Vi}sig\sum_{i=1}^{n}(\bar{\mathbf{e}}_{Pi} - \frac{\partial\gamma_{ij}^a}{\partial\mathbf{P}_i})^{\frac{1}{2}} \\
+ k_{2Vi}sign\sum_{i=1}^{n}(\bar{\mathbf{e}}_{Pi} - \frac{\partial\gamma_{ij}^a}{\partial\mathbf{P}_i}) + \dot{\mathbf{P}}_{d\,i} - \mathbf{e}_{Vi}] + \sum_{i=1}^{n}\mathbf{e}_{Vi}^T\mathbf{d}_{Vi}
\end{aligned}$$

$$\leq -k_{1Vi}\sum_{i=1}^{n}\sum_{m=1}^{3}|\bar{\mathbf{e}}_{Pim}-\frac{\partial\gamma_{ijm}^{a}}{\partial\mathbf{P}_i}|^{\frac{3}{2}}-k_{2Vi}||\sum_{i=1}^{n}(\bar{\mathbf{e}}_{Pi}-\frac{\partial\gamma_{ij}^{a}}{\partial\mathbf{P}_i})||$$
$$+||\sum_{i=1}^{n}(\bar{\mathbf{e}}_{Pi}-\frac{\partial\gamma_{ij}^{a}}{\partial\mathbf{P}_i})||(||\dot{\mathbf{P}}_{d\,i}||+||\mathbf{e}_{Vi}||)+\sum_{i=1}^{n}||\mathbf{e}_{Vi}||\,\|\mathbf{d}_{Vi}\|$$
$$\leq ||\sum_{i=1}^{n}(\bar{\mathbf{e}}_{Pi}-\frac{\partial\gamma_{ij}^{a}}{\partial\mathbf{P}_i})||(||\dot{\mathbf{P}}_{d\,i}||+||\mathbf{e}_{Vi}||)+\sum_{i=1}^{n}||\mathbf{e}_{Vi}||\,\|\mathbf{d}_{Vi}\| \tag{36}$$

According to the assumption 3, the derivative of desired trajectory $\|\dot{\mathbf{P}}_{d\,i}\|, i = 1, ..., n$ is bounded by l_1 and the disturbances $\mathbf{d}_{Vi}, i = 1, ..., n$ is bounded by l_2, $l_2 = \max\{k_{4Vi}\}$.

If $\|\mathbf{e}_{Vi}\| > 1$, we have $\|\mathbf{e}_{Vi}\| \leq \|\mathbf{e}_{Vi}\|^2 \leq 2\Phi_2$, the derivative of Φ_2 can be described as follows

$$\dot{\Phi}_2 \leq \frac{1}{2}l_1\Phi_2 + l_2\Phi_2 \leq \left(\frac{1}{2}l_1 + l_2\right)\Phi_2 \tag{37}$$

The above inequality means Φ_2 is bounded before the virtual velocity is traced at finite time. Therefore, $\|\mathbf{e}_{Vi}\|, \|\bar{\mathbf{e}}_{Pi}\|$ is bounded according to formula (37).

Lastly, the tracking to the desired trajectory for the virtual velocity will be proved. When the velocity error $\mathbf{e}_{Vi}$ converge to zero, the Lyapunov Φ_3 is given as follows

$$\Phi_3 = \frac{1}{2}\sum_{i=1,j=1,i\neq j}^{n}\left(\bar{\mathbf{e}}_{Pi}^{T}\bar{\mathbf{e}}_{Pi} + \gamma_{ij}^{a}\right) \tag{38}$$

Similarly, the derivative of Φ_3 is given as

$$\dot{\Phi}_3 \leq -k_{1Vi}\sum_{i=1}^{n}\sum_{m=1}^{3}\left|\bar{\mathbf{e}}_{Pim} - \frac{\partial\gamma_{ijm}^{a}}{\partial\mathbf{P}_i}\right|^{\frac{3}{2}}$$
$$-k_{2Vi}\left\|\sum_{i=1}^{n}\left(\bar{\mathbf{e}}_{Pi}-\frac{\partial\gamma_{ij}^{a}}{\partial\mathbf{P}_i}\right)\right\| + \left\|\sum_{i=1}^{n}\left(\bar{\mathbf{e}}_{Pi}-\frac{\partial\gamma_{ij}^{a}}{\partial\mathbf{P}_i}\right)\right\|\|\dot{\mathbf{P}}_{d\,i}\| \tag{39}$$

If $k_{2Vi} > \|\dot{\mathbf{P}}_{d\,i}\|$, we have

$$\dot{\Phi}_3 \leq -k_{1Vi}\sum_{i=1}^{n}\sum_{m=1}^{3}\left|\bar{\mathbf{e}}_{Pim} - \frac{\partial\gamma_{ijm}^{a}}{\partial\mathbf{P}_i}\right|^{\frac{3}{2}} \leq -\frac{k_{1Vi}}{2}(\Phi_3)^{\frac{3}{4}} \tag{40}$$

Therefore exists $\dot{\Phi}_3 < 0$, the trajectory tracking error$\mathbf{e}_{Pi}$ can converge to zero in finite-time.

5) STABILITY PROOF FOR THE ATTITUDE SYSTEM

Theorem 2: Consider system (1) satisfying Assumption 2, if the inner loop controller is designed as (30) while the derivative of $\zeta_{\Theta i}$ defined in (42) is bounded, then the sliding mode surface $\mathbf{s}_{\Theta i}$ and its derivative $\dot{\mathbf{s}}_{\Theta i}$ will converge to zero in finite-time and attitude tracking error $\mathbf{e}_{\Theta i}$ will converge to zero in finite-time.

Proof: Combined (29) and (30), the derivative of the sliding surface is obtained

$$\dot{\mathbf{s}}_{\Theta i} = -k_{1\Theta i}\frac{\mathbf{s}_{\Theta i}}{||\mathbf{s}_{\Theta i}||^{\frac{1}{2}}} - k_{2\Theta i}\mathbf{s}_{\Theta i} - \Pi(\boldsymbol{\Theta}_i)\mathbf{d}_{\Omega i} + \ddot{\boldsymbol{\Theta}}_{di} - \boldsymbol{\Theta}_{3ci}$$
$$+\int\left(-k_{3\Theta i}\frac{\mathbf{s}_{\Theta i}}{||\mathbf{s}_{\Theta i}||} - k_{4\Theta i}\mathbf{s}_{\Theta i}\right)dt \tag{41}$$

Define

$$\xi_{\Theta i} = \zeta_{\Theta i} + \int\left(-k_{3\Theta i}\frac{\mathbf{s}_{\Theta i}}{||\mathbf{s}_{\Theta i}||} - k_{4\Theta i}\mathbf{s}_{\Theta i}\right)dt$$
$$\zeta_{\Theta i} = -\boldsymbol{\Pi}(\boldsymbol{\Theta}_i)\mathbf{d}_{\Omega i} + \ddot{\boldsymbol{\Theta}}_{di} - \boldsymbol{\Theta}_{3ci}$$

The filter errors

$$\ddot{\boldsymbol{\Theta}}_{di} - \boldsymbol{\Theta}_{3ci} = \ddot{\boldsymbol{\Theta}}_{di} - \ddot{\boldsymbol{\Theta}}_{1ci} + \ddot{\boldsymbol{\Theta}}_{1ci} - \dot{\boldsymbol{\Theta}}_{2ci} + \dot{\boldsymbol{\Theta}}_{2ci} - \boldsymbol{\Theta}_{3ci}$$

are converge to zero after finite time according to reference [44], then (41) becomes

$$\dot{\mathbf{s}}_{\Theta i} = -k_{1\Theta i}\frac{\mathbf{s}_{\Theta i}}{||\mathbf{s}_{\Theta i}||^{\frac{1}{2}}} - k_{2\Theta i}\mathbf{s}_{\Theta i} + \xi_{\Theta i}$$
$$\dot{\xi}_{\Theta i} = -k_{3\Theta i}\frac{\mathbf{s}_{\Theta i}}{||\mathbf{s}_{\Theta i}||} - k_{4\Theta i}\mathbf{s}_{\Theta i} + \dot{\zeta}_{\Theta i} \tag{42}$$

According to Assumption 2, $\dot{\zeta}_{\Theta i}$ has a known bound. The candidate Lyapunov function Φ_4 is chosen as follows

$$\Phi_4 = 2k_{3\Theta i}\|\mathbf{s}_{\Theta i}\| + k_{4\Theta i}\mathbf{s}_{\Theta i}^{T}\mathbf{s}_{\Theta i} + \frac{1}{2}\xi_{\Theta i}^{T}\xi_{\Theta i} + \mathbf{J}_{2i}^{T}\mathbf{J}_{2i}$$
$$\triangleq \mathbf{J}_{2i}k_{1\Theta i}\frac{\mathbf{s}_{\Theta i}}{\|\mathbf{s}_{\Theta i}\|^{\frac{1}{2}}} + k_{2\Theta i}\mathbf{s}_{\Theta i} - \xi_{\Theta i} \tag{43}$$

According to [38], the inner loop attitude subsystem is finite time stable if controller parameters $k_{m\Theta i}, m = 1, 2, 3, 4$ choose suitably. Further, we have $e_{\Theta i} \to 0$ with the time of attitude tracking error in finite time.

Remark 1: The finite time convergence characteristics of the position outer and the attitude inner loop system are clarified. Considering the unmanned helicopters formation control problem, since the control frequency of the attitude inner loop is much shorter than the position outer loop, the principle of multi-time scale can be used to prove the finite time stability for the entire closed-loop system.

Remark 2: The parameters of the tracking controller are determined based on Theorem 1 and 2. Moreover, in the simulation, we have tried several groups of data and selected better parameters.

Remark 3: The innovation of this paper is to design a virtual speed tracking controller (19) with collision avoidance, and prove the finite-time formation reconfiguration control.

IV. SIMULATION

Assume that in the process of formation generation, 10 unmanned helicopters take off from the ground, form a flight formation in three-dimensional space. The simulation is conducted on a computer with i5-2450M @2.5GHz processor and 8 GB of RAM.

Firstly, the model and controller parameters of the specific helicopters used in the simulation are given in **Table 1** and **Table 2**. Among them, the UAV model parameters including helicopter mass, gravity acceleration, proportional coefficient, moment of inertia matrix and multiple coefficient matrices are given.

TABLE 1. The parameter value of model variables.

variables	values
m	$8.2kg$
g	$9.81m/s^2$
Z_w^i	$-0.7615s^{-1}$
Z_{col}^i	$-131.4125m/(\text{rad}\cdot s^2)$
$\mathbf{J}_i$	$\begin{bmatrix}0.18 & 0 & 0\\ 0 & 0.34 & 0\\ 0 & 0 & 0.28\end{bmatrix} kg\cdot m^2$
$\mathbf{A}_i$	$\begin{bmatrix}-48.1757 & 0 & 0\\ 0 & -25.5048 & 0\\ 0 & 0 & -0.9808\end{bmatrix} s^{-1}$
$\mathbf{B}_i$	$\begin{bmatrix}0 & 1689.5 & 135.8\\ 894.5 & 0 & 0\\ 0 & 0 & 135.8\end{bmatrix} s^{-2}$
N_{col}^i	$-0.3705\,s^{-2}$

TABLE 2. The parameter value of controller.

variables	values
k_{1Vi}	1
k_{2Vi}	0.001
k_{3Vi}	1
k_{4Vi}	1
β_{2i}	1
$k_{1\Theta i}$	0.001
$k_{2\Theta i}$	18
$k_{3\Theta i}$	0.001
$k_{4\Theta i}$	18
r_a	8

The initial velocity, attitude angle, and attitude angular velocity are all zero, and the initial positions of each unmanned helicopter are set as

$$P_1(0) = [0, 240, 0]^T m,\ P_2(0) = [0, 250, 0]^T m,$$
$$P_3(0) = [10, 250, 0]^T m,\ P_4(0) = [250, 10, 0]^T m,$$
$$P_5(0) = [240, 10, 0]^T m,\ P_6(0) = [250, 0, 0]^T m,$$
$$P_7(0) = [240, 0, 0]^T m,\ P_8(0) = [0, 0, 0]^T m,$$
$$P_9(0) = [10, 0, 0]^T m,\ P_{10}(0) = [0, 10, 0]^T m.$$

Consider that the model parameters are uncertain, the mass and moment of inertia are biased by 30%, and the external wind disturbance is simulated as constant wind and sinusoidal wind which is given by

$$\mathbf{d}_{Vi} = \begin{bmatrix}20(1+\sin(t)+\cos(t))\Delta m_i\\ 15(1.5+\sin(2t)+\cos(1.5t))\Delta m_i\\ 18(1+1.5\sin(t)+2\cos(t))\Delta m_i\end{bmatrix},\ \Delta m_i = 0.3m_i$$

$$\mathbf{d}_{\Omega i} = \begin{bmatrix}0.1(1+\sin(t)+\cos(t))\Delta J_i\\ 0.07(1+\sin(3t)+\cos(2t))\Delta J_i\\ 0.09(1+0.8\sin(t)+0.7\cos(t))\Delta J_i\end{bmatrix},\ \Delta J_i = 0.3J_i$$

The simulation results are given as follows:

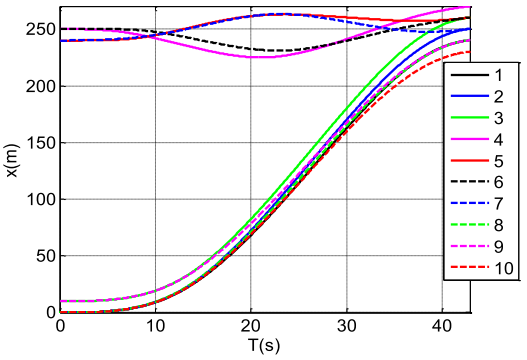

FIGURE 4. Desired position in the x direction.

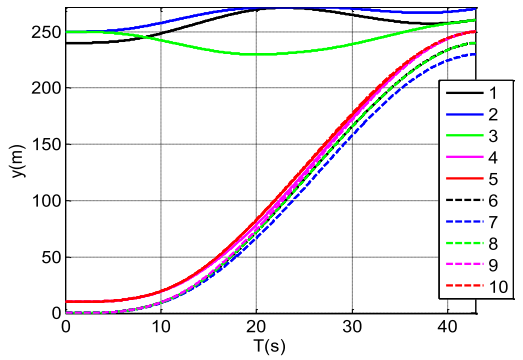

FIGURE 5. Desired Position in the y direction.

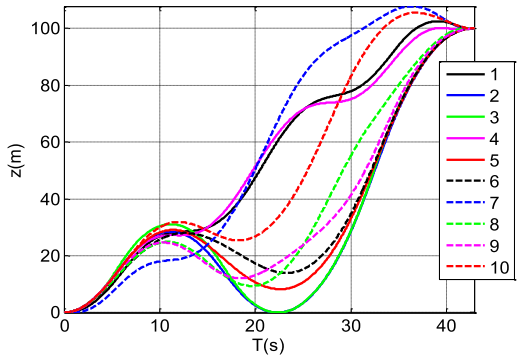

FIGURE 6. Desired Position in the y direction.

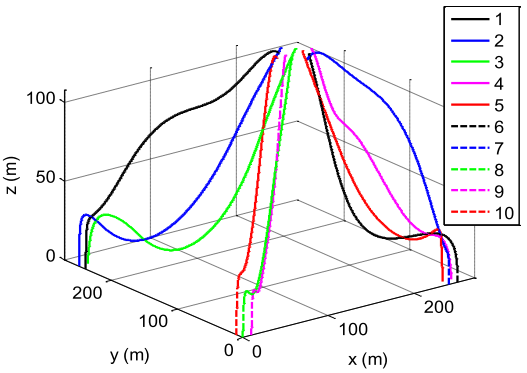

FIGURE 7. Trajectories for 10 unmanned helicopters.

From **FIGURE 4** to **FIGURE 6**, the desired position in the x, y, z direction are given, it can be seen that 10 unmanned

helicopters reach the desired position at the same time and the desired position has a gentle changes with time in the range of [0, 300] m which satisfies the constraints(5).

In the simulation, the computation time for RRT method is compared with the PSO and ACO method. As shown in **TABLE 3**, the RRT method has 10 times faster than the PSO method and 4000 times faster than the ACO method. From the simulation, the RRT and PSO method can be used in the real-time environment and the RRT method has a faster convergence speed. The ACO method could only be used in the offline computation.

TABLE 3. The computation time comparison.

method	Computation time
PSO	1s
ACO	400s
RRT	0.1s

As shown in **FIGURE 7**, a schematic diagram of the trajectories of 10 unmanned helicopters formation is given. It can be seen that the trajectory changes are gentle and the effect is good. In the current simulation environment, as shown in, the computation time of the pseudospectral method without the RRT algorithm is about 10s. By comparision, the optimal path point computation time of RRT algorithm is about 0.1s, and the time for the pseudospectral method to solve the optimal trajectory of 10 unmanned helicopters formation is about 0.9s. In general, the whole computation time is about 1s which meets the real-time requirements perfectly. Thus, the calculation efficiency can be increased by 10 times for 10 unmanned helicopters formation generation problem through the proposed method in this paper.

TABLE 4. The parameter value of model variables.

method	Computation time
Pseudospectral method	10s
Pseudospectral+RRT method	0.9s+0.1s=1s

The tracking control results of 10 unmanned helicopters formation are shown in Figure 8-13.

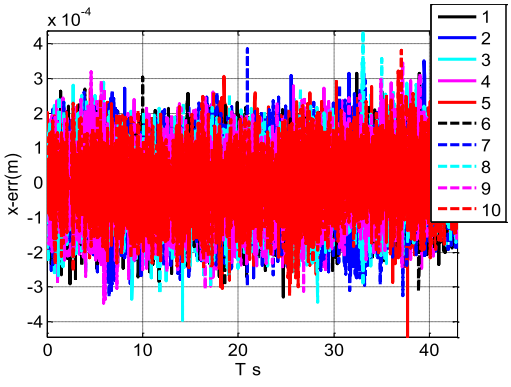

FIGURE 8. Position error in the x direction.

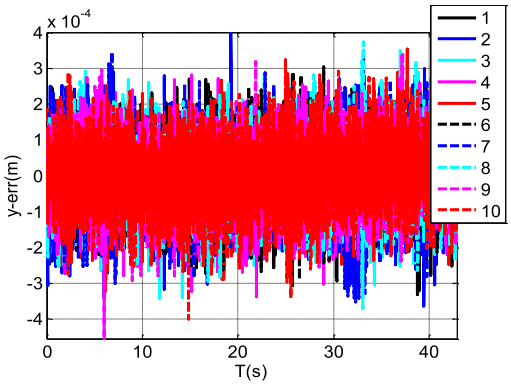

FIGURE 9. Position error in the y direction.

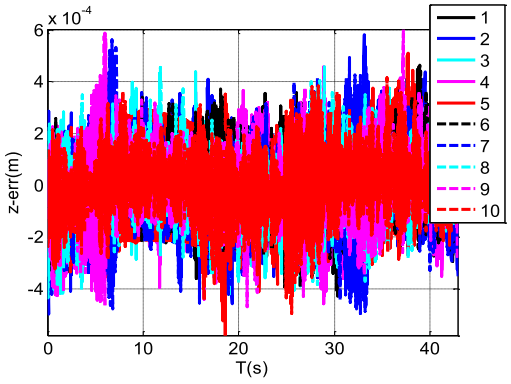

FIGURE 10. Position error in the z direction.

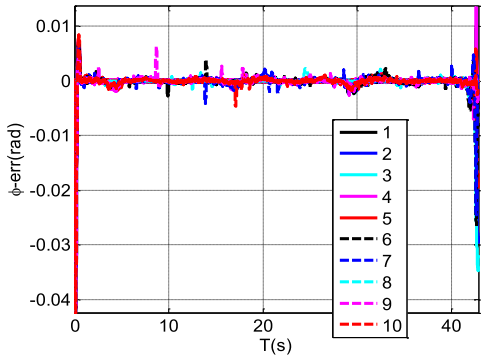

FIGURE 11. Attitude error in the ϕ direction.

From **FIGURE 8** to **FIGURE 10**, the tracking errors of the formation trajectory of the formation are shown. Under the influence of external disturbance and uncertainty, the trajectory tracking control error of the UAV formation is 10^{-4}m. It means that the proposed finite-time controller satisfies the requirements of high-precision control, and at the same time in the trajectory tracking part, the convergence time is small and can be ignored.

From **FIGURE 11** to **FIGURE 13**, the variation trend of the attitude error with time in the formation process of 10 UAV formations is given. From the figures, it can be seen that under the influence of external disturbance and uncertainty, in the existing simulation environment, the attitude control error in the θ and ϕ direction of the UAV

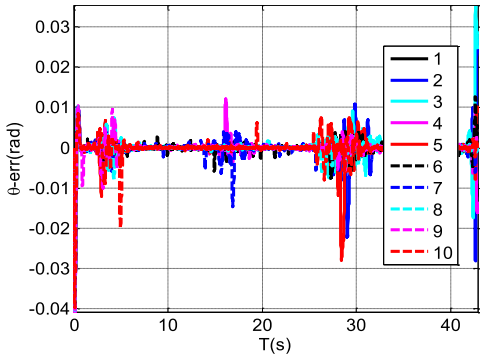

FIGURE 12. Attitude error in the θ direction.

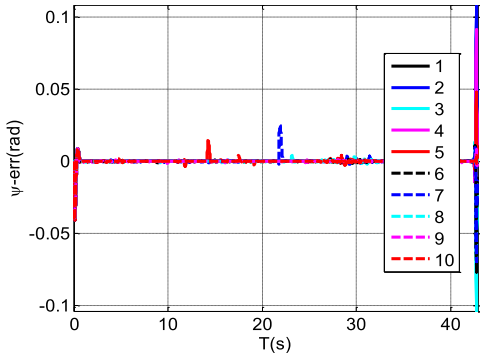

FIGURE 13. Attitude error in the ψ direction.

formation attitude tracking is within 0.04 rad; the attitude control error in the ψ direction of the UAV formation attitude tracking is within 0.11 rad, considering the position error in the final time, which satisfies the control requirements of the entire closed-loop system.

V. CONCLUSION

In this paper, a novel safe formation generation strategy is proposed for the multiple unmanned helicopters through trajectory optimization and tracking control. Firstly, to reduce the computation time, pseudospectral method and a NLP solver are used to obtain the optimal trajectory during which the RRT algorithm is applied to obtain the initial guess. Then, to ensure the finite time trajectory tracking in the presence of model parameter uncertainties and unknown external disturbances, a finite-time sliding mode controller is proposed through terminal sliding mode method and potential energy function approach. Finally, the efficiency of the proposed strategy is illustrated by numerical simulation.

REFERENCES

[1] S. J. Levulis, P. R. DeLucia, and S. Y. Kim, "Effects of touch, voice, and multimodal input, and task load on multiple-UAV monitoring performance during simulated manned-unmanned teaming in a military helicopter," *Hum. Factors*, vol. 60, no. 8, pp. 1117–1129, 2018.

[2] G. Barbarosoğlu, L. Özdamar, and A. Çevik, "An interactive approach for hierarchical analysis of helicopter logistics in disaster relief operations," *Eur. J. Oper. Res.*, vol. 140, no. 1, pp. 118–133, 2002.

[3] V. N. Nguyen, R. Jenssen, and D. Roverso, "Automatic autonomous vision-based power line inspection: A review of current status and the potential role of deep learning," *Int. J. Elect. Power Energy Syst.*, vol. 99, pp. 107–120, Jul. 2018.

[4] Y. Bae and Y. M. Koo, "Flight attitudes and spray patterns of a roll-balanced agricultural unmanned helicopter," *Appl. Eng. Agricult.*, vol. 29, no. 5, pp. 675–682, 2013.

[5] X. Wang and X. Zhao, "A practical survey on the flight control system of small-scale unmanned helicopter," in *Proc. IEEE 7th World Congr. Intell. Control Automat. (WCICA)*, Jun. 2008, pp. 364–369.

[6] O. von Stryk and R. Bulirsch, "Direct and indirect methods for trajectory optimization," *Ann. Oper. Res.*, vol. 37, no. 1, pp. 357–373, 1992.

[7] R. Bulirsch, E. Nerz, O. von Stryk, and H. J. Pesch, "Combining direct and indirect methods in optimal control: Range maximization of a hang glider," in *Optimal Control*. Basel, Switzerland: Birkhäuser, 1993, pp. 273–288.

[8] M. Pontani and B. A. Conway, "Minimum-fuel finite-thrust relative orbit maneuvers via indirect heuristic method," *J. Guid., Control, Dyn.*, vol. 38, no. 5, pp. 913–924, 2014.

[9] R. L. Barron and C. M. Chick, "Trim-reference functions for indirect method of trajectory optimization," *J. Guid., Control, Dyn.*, vol. 30, no. 4, pp. 1189–1193, 2007.

[10] T. Grüning, A. Rauh, and H. Aschemann, "Feedforward control design for a four-rotor UAV using direct and indirect methods," in *Proc. IEEE 17th Int. Conf. Methods Models Automat. Robot. (MMAR)*, Aug. 2012, pp. 439–444.

[11] T. Liu, Y. S. Zhao, B. J. Li, and P. Shi, "Trajectory optimization for spacecraft proximity rendezvous using direct collocation method," *Adv. Mater. Res.*, vols. 433–440, pp. 6652–6656, Jan. 2012.

[12] T. Jiang, J. Li, K. Huang, C. Yang, Y. Jiang, and B. Li, "Trajectory optimization for a cruising unmanned aerial vehicle attacking a target at back slope while subjected to a wind gradient," *Math. Problems Eng.*, vol. 2015, Jun. 2015, Art. no. 635395.

[13] Z. Yu, C. Jing, and S. Lincheng, "Real-time trajectory planning for UCAV air-to-surface attack using inverse dynamics optimization method and receding horizon control," *Chin. J. Aeronautics*, vol. 26, no. 4, pp. 1038–1056, 2013.

[14] I. M. Ross, P. Sekhavat, Q. Gong, and A. Fleming, "Optimal feedback control: Foundations, examples, and experimental results for a new approach," *J. Guid., Control, Dyn.*, vol. 31, no. 2, pp. 307–321, 2008.

[15] G. T. De Azevedo, P. A. Q. De Assis, R. K. H. Galvão, and V. P. Pinto, "Pseudospectral optimisation of UAV trajectories for minimal battery consumption in the presence of a wind field," in *Proc. IEEE UKACC 12th Int. Conf. Control (CONTROL)*, Sep. 2018, pp. 272–276.

[16] D. J. Grymin and M. Farhood, "Two-step system identification and trajectory tracking control of a small fixed-wing UAV," *J. Intell. Robot. Syst.*, vol. 83, no. 1, pp. 105–131, 2016.

[17] K. Tang, B. Wang, B. Chen, and W. Kang, "Minimum time control of helicopter UAVs using computational dynamic optimization," in *Proc. 9th IEEE Int. Conf. Control Automat. (ICCA)*, Dec. 2011, pp. 848–852.

[18] B. Zhang, Q. Zong, S. Shao, and H. C. Lu, "Trajectory optimization of quad-rotor UAV formation using hp-adaptive pseudospectral method," *Sci. Sinica Technol.*, vol. 47, no. 3, pp. 239–248, 2017.

[19] C. YongBo, M. YueSong, S. XiaoLong, X. Nuo, and Y. JianQiao, "Three-dimensional unmanned aerial vehicle path planning using modified wolf pack search algorithm," *Neurocomputing*, vol. 266, pp. 445–457, Nov. 2017.

[20] R. Chai, A. Savvaris, and A. Tsourdos, "Violation learning differential evolution-based hp-adaptive pseudospectral method for trajectory optimization of space maneuver vehicle," *IEEE Trans. Aerosp. Electron. Syst.*, vol. 53, no. 4, pp. 2031–2044, Aug. 2017.

[21] Y.-J. Tsai, C.-S. Lee, C.-L. Lin, and C.-H. Huang, "Development of flight path planning for multirotor aerial vehicles," *Aerospace*, vol. 2, no. 2, pp. 171–188, 2015.

[22] Z. Liu, Y. Zhang, L. Ciarletta, D. Theilliol, and C. Yuan, "Collision avoidance and path following control of unmanned aerial vehicle in hazardous environment," *J. Intell. Robot. Syst.*, vol. 95, no. 1, pp. 193–210, Jul. 2019.

[23] G. Y. Yin, S. L. Zhou, and Q. P. Wu, "An improved RRT algorithm for UAV path planning," *Acta Electron. Sinica*, vol. 45, no. 7, pp. 1764–1769, 2017.

[24] P. K. Das, H. S. Behera, and B. K. Panigrahi, "A hybridization of an improved particle swarm optimization and gravitational search algorithm for multi-robot path planning," *Swarm Evol. Comput.*, vol. 28, pp. 14–28, Jun. 2016.

[25] A. Lazarowska, "Ship's trajectory planning for collision avoidance at sea based on ant colony optimisation," *J. Navigat.*, vol. 68, no. 2, pp. 291–307, 2015.
[26] G. Cai, B. Chen, X. Dong, and T. H. Lee, "Design and implementation of a robust and nonlinear flight control system for an unmanned helicopter," *Mechatronics*, vol. 21, no. 5, pp. 803–820, 2011.
[27] Y. He and J. Han, "Decentralized receding horizon control for multiple unmanned helicopters considering dynamics model," in *Proc. 48h IEEE Conf. Decis. Control (CDC), Held Jointly 28th Chin. Control Conf.*, Dec. 2009, pp. 8351–8356.
[28] A. Karimoddini, H. Lin, T. H. Lee, and B. M. Chen, "A bumpless hybrid supervisory control algorithm for the formation of unmanned helicopters," *Mechatronics*, vol. 23, no. 6, pp. 677–688, 2013.
[29] J. Ghommam, L. F. Luque-Vega, M. Saad, and B. Castillo-Toledo, "Three-dimensional distributed tracking control for multiple quadrotor helicopters," *J. Franklin Inst.*, vol. 353, no. 10, pp. 2344–2372, 2016.
[30] J.-J. Xiong and E.-H. Zheng, "Position and attitude tracking control for a quadrotor UAV," *ISA Trans.*, vol. 53, no. 3, pp. 725–731, 2014.
[31] B. Tian, J. Cui, H. Lu, Z. Zuo, and Q. Zong, "Adaptive finite-time attitude tracking of quadrotors with experiments and comparisons," *IEEE Trans. Ind. Electron.*, to be published. doi: 10.1109/TIE.2019.2892698.
[32] B. Tian, L. Liu, H. Lu, Z. Zuo, Q. Zong, and Y. Zhang, "Multivariable finite time attitude control for quadrotor UAV: Theory and experimentation," *IEEE Trans. Ind. Electron.*, vol. 65, no. 3, pp. 2567–2577, Mar. 2018.
[33] B. Tian, L. Yin, and H. Wang, "Finite-time reentry attitude control based on adaptive multivariable disturbance compensation," *IEEE Trans. Ind. Electron.*, vol. 62, no. 9, pp. 5889–5898, Sep. 2015.
[34] B. Tian, W. Fan, R. Su, and Q. Zong, "Real-time trajectory and attitude coordination control for reusable launch vehicle in reentry phase," *IEEE Trans. Ind. Electron.*, vol. 62, no. 3, pp. 1639–1650, Mar. 2015.
[35] B. Tian, Z. Zuo, H. Wang, and X. Yan, "A fixed-time output feedback control scheme for double integrator systems," *Automatica*, vol. 80, pp. 17–24, Jun. 2017.
[36] B. Xu, "Composite learning finite-time control with application to quadrotors," *IEEE Trans. Syst., Man, Cybern., Syst.*, vol. 48, no. 10, pp. 1806–1815, Oct. 2018.
[37] H. Yang, H. Lin, J. Zeng, and J. Wang, "Flight control of tilt rotor UAV during transition mode based on finite-time control theory," in *Proc. Euro-China Conf. Intell. Data Anal. Appl.* Cham, Switzerland: Springer, 2018, pp. 65–77.
[38] B. Tian, H. Lu, Q. Zong, Y. Zhang, and Z. Zuo, "Multivariable finite-time output feedback trajectory tracking control of quadrotor helicopters," *Int. J. Robust Nonlinear Control*, vol. 28, no. 1, pp. 281–295, 2018.
[39] H. Duan, Q. Luo, G. Ma, and Y. Shi, "Hybrid particle swarm optimization and genetic algorithm for multi-UAV formation reconfiguration," *IEEE Comput. Intell. Mag.*, vol. 8, no. 3, pp. 16–27, Aug. 2013.
[40] L. Sauter and P. Palmer, "Onboard semianalytic approach to collision-free formation reconfiguration," *IEEE Trans. Aerosp. Electron. Syst.*, vol. 48, no. 3, pp. 2638–2652, Jul. 2012.
[41] J. Sun, J. Tang, and S. Lao, "Collision avoidance for cooperative UAVs with optimized artificial potential field algorithm," *IEEE Access*, vol. 5, pp. 18382–18390, 2017.
[42] D. V. Dimarogonas, "Sufficient conditions for decentralized potential functions based controllers using canonical vector fields," *IEEE Trans. Autom. Control*, vol. 57, no. 10, pp. 2621–2626, Oct. 2012.
[43] A. H. Qureshi and Y. Ayaz, "Potential functions based sampling heuristic for optimal path planning," *Auto. Robots*, vol. 40, no. 6, pp. 1079–1093, Aug. 2016.
[44] D. Wang, Q. Zong, S. Shao, X. Zhang, X. Zhao, and B. Tian, "Neural network disturbance observer-based distributed finite-time formation tracking control for multiple unmanned helicopters," *ISA Trans.*, vol. 73, pp. 208–226, Feb. 2018.
[45] D. Wang, B. Tian, F. Wang, L. Dou, and Q. Zong, "Finite-time fully distributed formation reconfiguration control for UAV helicopters," *Int. J. Robust Nonlinear Control*, vol. 28, no. 18, pp. 5943–5961, 2018.
[46] D. Wang, B. Tian, H. Lu, J. Wang, and Q. Zong, "Adaptive finite-time reconfiguration control of unmanned aerial vehicles with a moving leader," *Nonlinear Dyn.*, vol. 95, no. 2, pp. 1099–1116, 2019.
[47] I. Nagesh and C. Edwards, "A multivariable super-twisting sliding mode approach," *Automatica*, vol. 50, pp. 984–988, Mar. 2014.

BOYUAN ZHANG received the bachelor's degrees in automatic control from Dalian Maritime University, China, in 2016. He is currently pursuing the Ph.D. degree with the School of Electrical and Electronic Engineering, Tianjin University. His main research is trajectory optimization and flight control.

QUN ZONG (M'04) received the bachelor's, master's, and Ph.D. degrees in automatic control from Tianjin University, Tianjin, China, in 1983, 1988, and 2002, respectively, where he is currently a Professor with the School of Electrical and Information Engineering. His main research interests include complex system modeling and flight control.

LIQIAN DOU received the B.S., M.S., and Ph.D. degrees in automatic control from Tianjin University, Tianjin, China, in 1999, 2005, and 2008, respectively. He was an Academic Visitor with the School of Electrical and Electronic Engineering, University of Manchester, Manchester, U.K., from 2015 to 2016. He is currently an Associate Professor with the School of Electrical and Information Engineering, Tianjin University, Tianjin. His main research interests include coordinate control of multi-UAVs.

BAILING TIAN (M'11) received the B.S., M.S., and Ph.D. degrees in automatic control from Tianjin University, Tianjin, China, in 2006, 2008, and 2011, respectively. He was an Academic Visitor with the School of Electrical and Electronic Engineering, University of Manchester, Manchester, U.K., from 2014 to 2015. He is currently an Associate Professor with the School of Electrical and Information Engineering, Tianjin University. His main research interests include finite time control, and integrated guidance and control for vehicles.

DANDAN WANG received the M.S. degree in mathematics from Qufu Normal University, Qufu, China, in 2015. She is currently pursuing the Ph.D. degree with Tianjin University, Tianjin, China. Her current research interests include multiUAV formation control, event-triggered consensus control, and stability analysis of the impulsive and switching system with time delay.

XINYI ZHAO received the B.S. degrees in automatic control from Tianjin University, Tianjin, China, in 2015, where she is currently pursuing the Ph.D. degree with the School of Electrical and Electronic Engineering. Her main research interests are intelligent planning and control.